Supplementary Material for FSAD-Net: Feedback Spatial Attention Dehazing Network

***Abstract*—This supplementary document provides experiments, which could not be fit in the paper due to page limit.**

I. Experiments on Real Data

In this section, we provide more dehazed results on real-world images. To evaluate our proposed dehazing method on natural hazy images, we evaluate 6 representative state-of-the-art algorithms: DCP [1], LPQC [2], PDN [3], GFN [4], DDIP [5], and cGAN [6]. For the hazy images of natural scenes, we mainly compare the dehazing performance, the preservation of details and the colour distortion of different algorithms from the visual perspective. Fig. 1 show the comparison on natural haze images. The DCP [1], PDN [3], DDIP [5] suffer severe color distortions. For LPQC [2], haze removal is clearly incomplete. The GFN [4] and cGAN [6] have limited abilities to deal with distant region and cause color distortions in some cases (e.g., the red box indicated in Fig. 1 looks darker). In comparison to the aforementioned methods, our FSAD-Net is more effective in haze removal and distortion suppression.

II. Experiments on Synthetic Data

Fig. 2 shows some examples of our synthetic training data. Table I shows the quantitative analysis of single image haze removal on NTIRE database [7]. Compared with the state-of-the-arts, the proposed method has the best performance in terms of PSNR, and it prove that our FSAD-Net is fairly robust and continues to show highly competitive performance. Fig. 3 show the visual results on NTIRE [7].

In the main paper, we evaluate our method on the HazeRD [8] to better represent our method is robust to the diversity of the haze scenarios. Here we present more visual results on HAZERD [8] in Fig. 4. Our method generates cleaner results with less artifacts and color distortion.

We also present the comparisons on outdoor synthetic haze images. The methods used for comparisons including DCP [1], HL [9], LPQC [2], PDN [3], GFN [4], DDIP [5], cGAN [6], and FD-GAN [10]. It can be seen from Fig. 5 that all methods can remove the haze, but the color fidelity of the sky region is different. Compared with the results of using the other eight methods, our method achieves the best color fidelity and generates more haze-clear results in Fig. 5(j).

III. Ablation Study

We conducted ablations on the components of the FSAD-Net architecture, and showed the quantitative comparisons in the main paper. Here we present visual dehazed results in Fig. 6. The visual results show that all these network designs are crucial to the performance of the proposed model.

TABLE I: Average PSNR comparison on the NTIRE [7]. Bold font is used for indicating our results.

Methods	Indoor	Outdoor	Average
DCP [1]	16.71	17.46	17.09
HL [9]	17.30	16.43	16.87
AOD-Net [11]	16.90	17.28	17.09
GFN [4]	17.28	17.11	17.19
DDIP [5]	16.78	15.69	16.24
Ours FSAD-Net	**17.00**	**17.77**	**17.38**

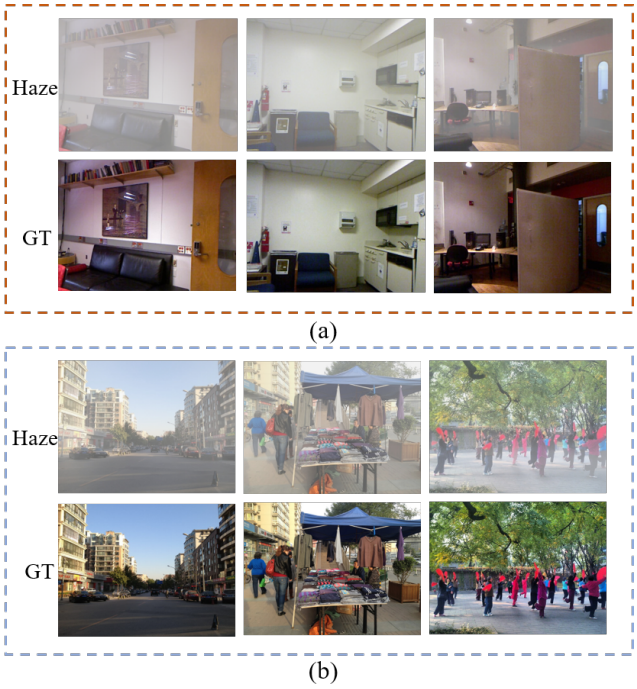

Fig. 2: Examples in our synthetic training data. (a) Synthetic indoor images. (b) Synthetic outdoor images.

Besides, we analyzed the effect of spatial attention block (SAB) and feedback block (FB) on the SOTS dataset, and showed the quantitative comparisons and qualitative comparisons in the main paper. To further prove performances of the SAB and FB, we conduct the quantitative and qualitative comparisons on HAZERD [8] dataset. The quantitative results are shown in Table II and Table III. The visual comparisons are shown in Fig. 7 and Fig. 8.

Fig. 1: Qualitative comparison of different methods on real-world images. Our FSAD-Net is more effective in haze removal and distortion suppression.

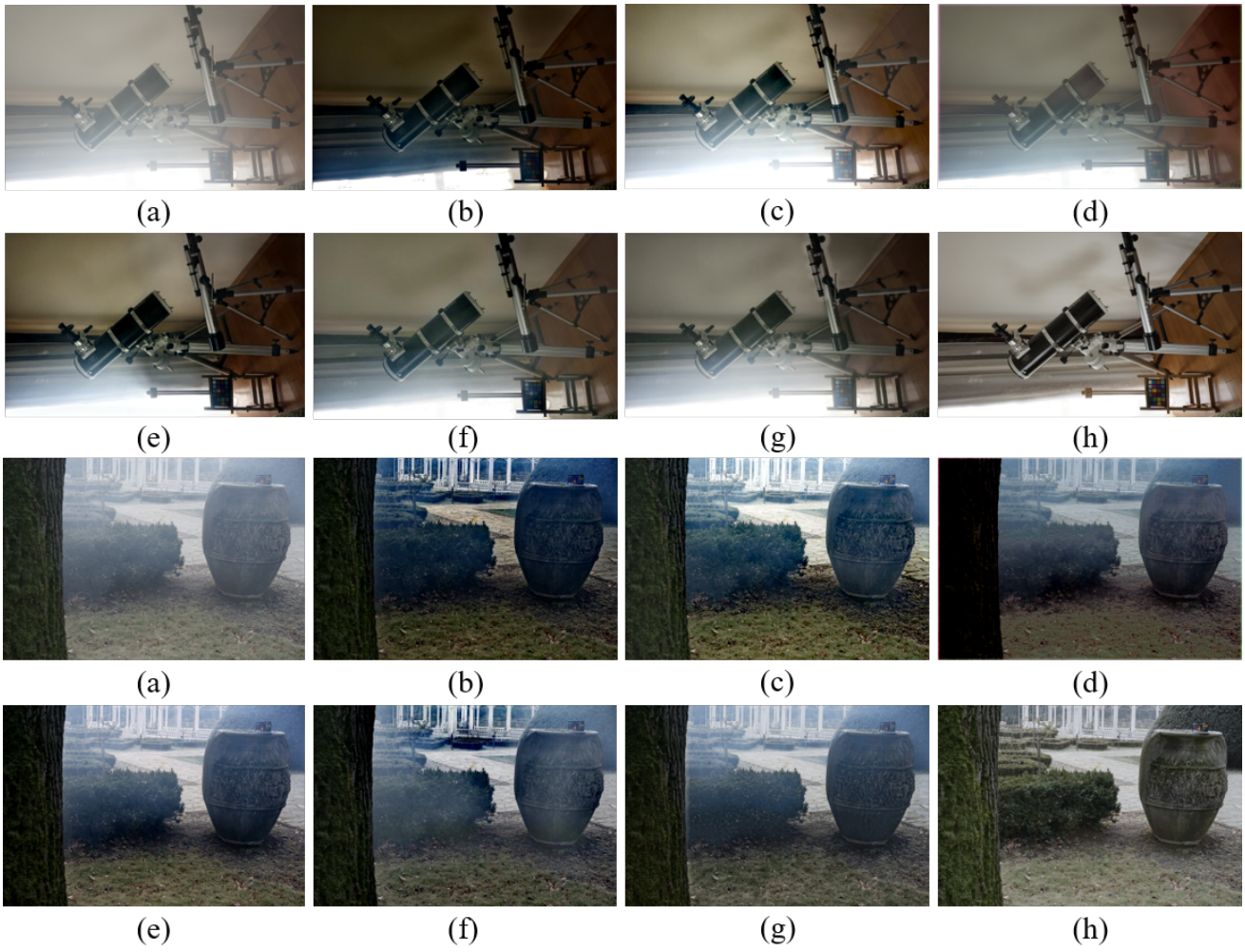

Fig. 3: Qualitative comparison of different methods on the NTIRE [7]. (a) Haze image, haze-free images restored by (b) DCP [1], (c) HL [9], (d) AOD-Net [11], (e) GFN [4], (f) DDIP [5], and (g) our FSAD-Net. (k) Ground truths.

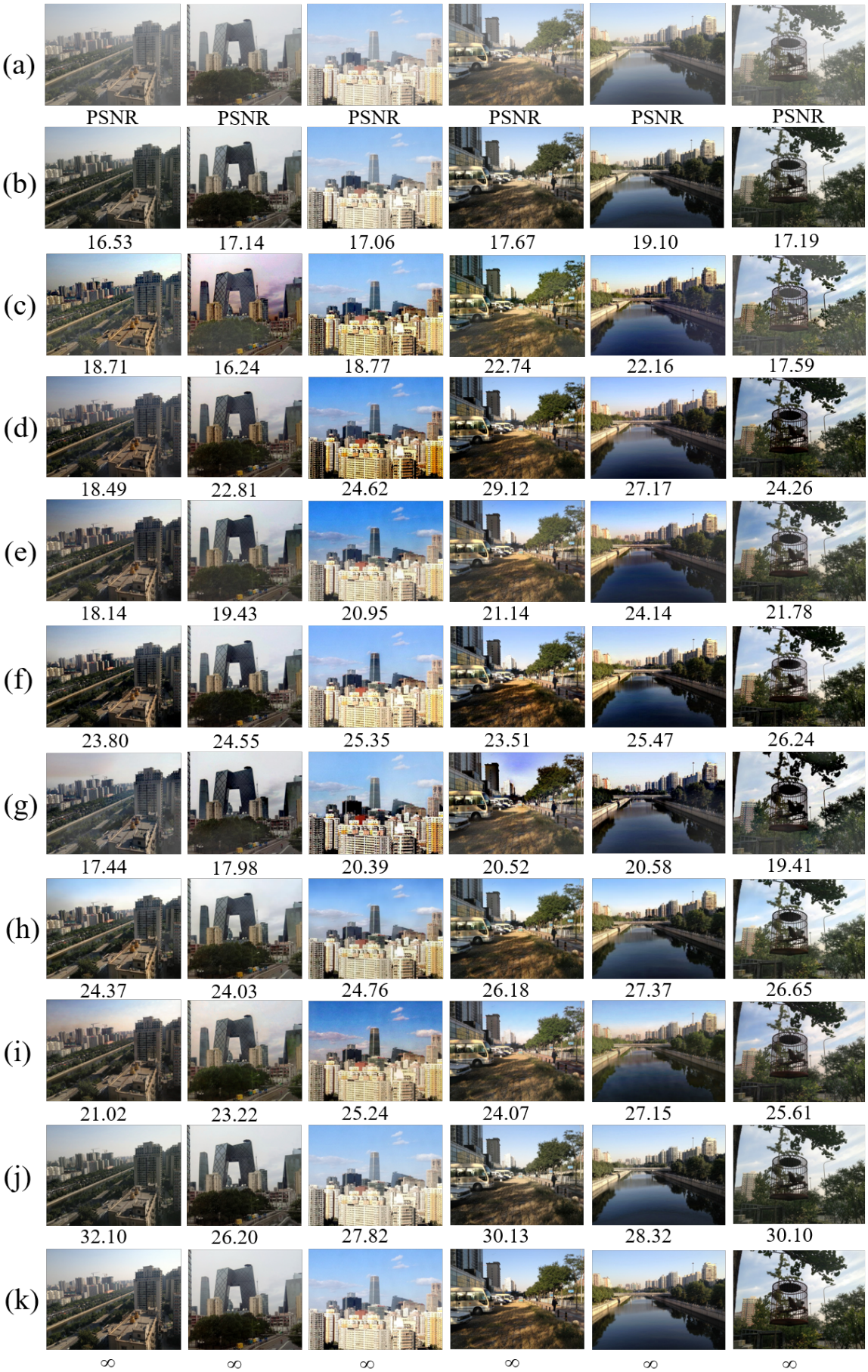

Fig. 5: Qualitative comparison of different methods on synthetic outdoor image. (a) Haze image, haze-free images restored by (b) DCP [1], (c) HL [9], (d) LPQC [2], (e) PDN [3], (f) GFN [4], (g) DDIP [5], (h) cGAN [6], (i) FD-GAN [10], and (j) our FSAD-Net. (k) Ground truths.

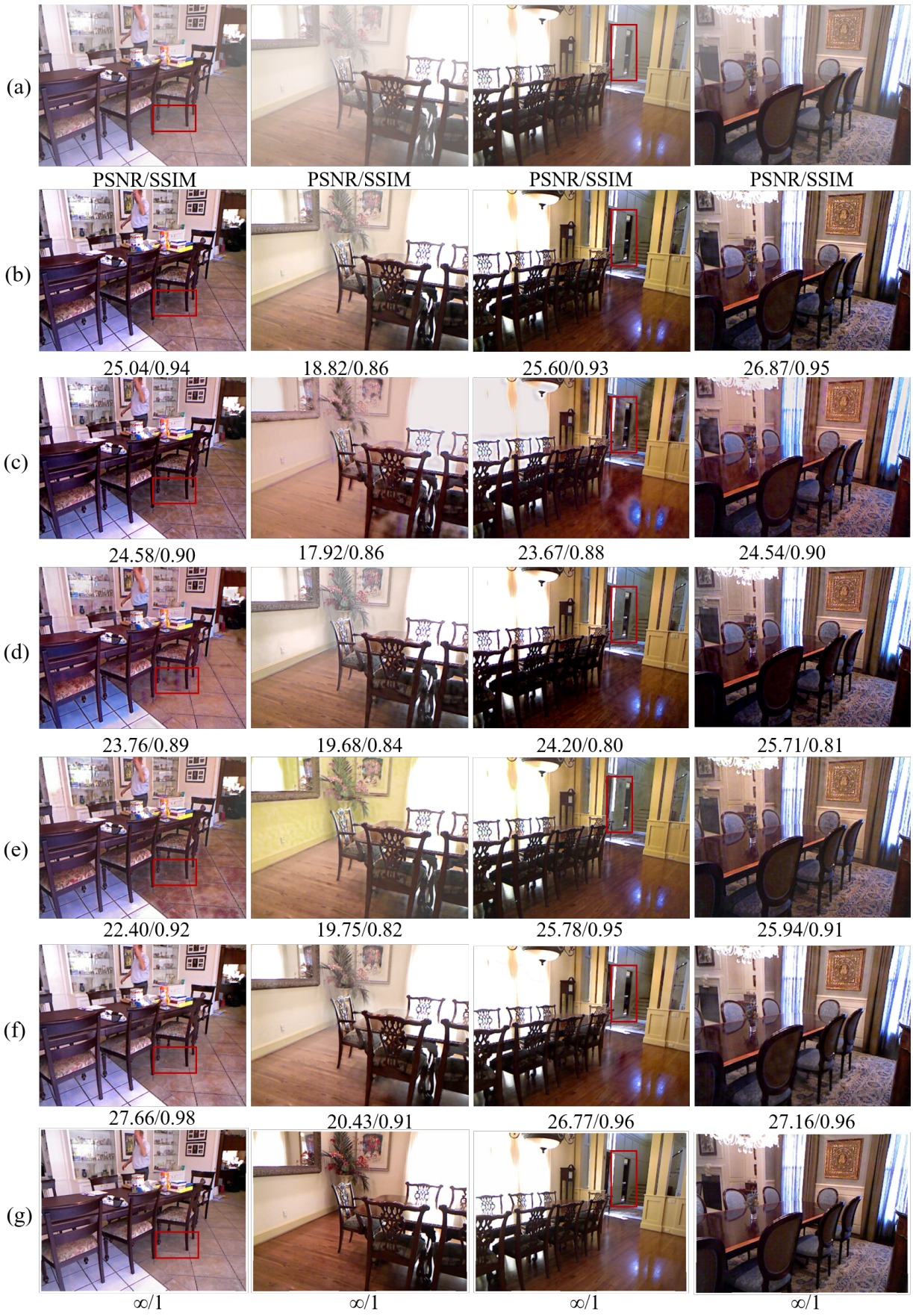

Fig. 6: Comparisons on SOTS indoor images for different configurations. (a) Haze image, haze-free images restored by (b) FSAD-Net without feedback block and multistage iterations, (c) FSAD-Net without mechanism and skip fusion, (d)FSAD-Net without feedback block, (e) FSAD-Net without multistage iterations, (f) our FSAD-Net. (g) Ground truths.

(a) Input image (b) Only LSTM (c) Only GRU (d) our FSAD-Net (e) Ground truth

Fig. 8: Comparison results of FSAD-Net models with different feedback blocks in visual effect on HAZERD [8] dataset. Our FSAD-Net has less haze remaining and generates images with vivid colors.

TABLE II: Quantitative results on FSAD-Net models with and without spatial attention block. We evaluate the PSNR and SSIM on the HAZERD [8] dataset. Bold font is used for indicating best results.

Methods	w/o attention	our FSAD-Net
PSNR	17.5997	**17.8144**
SSIM	0.5431	**0.5889**

TABLE III: Average PSNR and SSIM comparison of FSAD-Net models with different feedback blocks on the HAZERD [8]. Bold font is used for indicating best results.

Methods	Only LSTM	Only GRU	our FSAD-Net
PSNR	17.5452	16.1143	**17.8144**
SSIM	0.4003	0.5765	**0.5889**

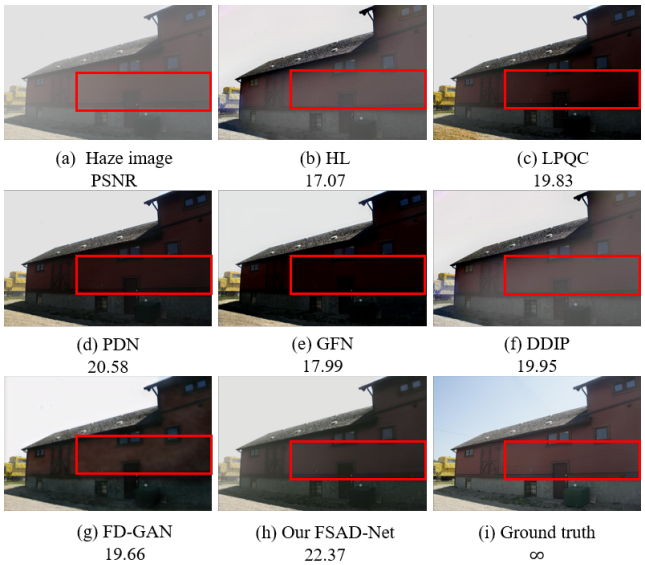

(a) Haze image PSNR (b) HL 17.07 (c) LPQC 19.83

(d) PDN 20.58 (e) GFN 17.99 (f) DDIP 19.95

(g) FD-GAN 19.66 (h) Our FSAD-Net 22.37 (i) Ground truth ∞

Fig. 4: Qualitative comparison of different methods on HAZERD [8] dataset. (a) Haze images. Dehazing results by (b) HL [9], (c) LPQC [2], (d) PDN [3], (e) GFN [4], (f) DDIP [5], (g) FD-GAN [10], and (h) our FSAD-Net. (i) Ground truth.

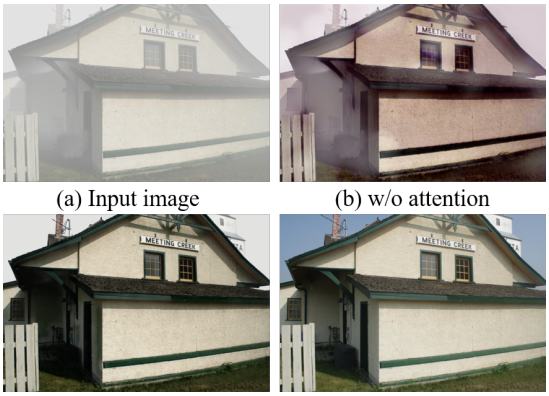

(a) Input image (b) w/o attention

(c) our FSAD-Net (d) Ground truth

Fig. 7: Comparison of FSAD-Net with and without spatial attention in visual effects on HAZERD dataset [8]. Our FSAD-Net has less haze remaining and is close to ground truth.

REFERENCES

[1] K. He, J. Sun, and X. Tang, "Single image haze removal using dark channel prior," *IEEE TPAMI*, vol. 33, no. 12, pp. 2341–2353, 2011.

[2] S. Santra, R. Mondal, and B. Chanda, "Learning a patch quality comparator for single image dehazing," *IEEE TIP*, vol. 27, no. 9, pp. 4598–4607, 2018.

[3] D. Yang and J. Sun, "Proximal dehaze-net: A prior learning-based deep network for single image dehazing," in *ECCV*, 2018, pp. 729–746.

[4] W. Ren, L. Ma, J. Zhang, J. Pan, X. Cao, W. Liu, and M.-H. Yang, "Gated fusion network for single image dehazing," in *IEEE CVPR*, 2018, pp. 3253–3261.

[5] Y. Gandelsman, A. Shocher, and M. Irani, ""Double-DIP": Unsupervised image decomposition via coupled deep-image-priors," in *IEEE CVPR*, 2019, pp. 11 018–11 027.

[6] R. Li, J. Pan, Z. Li, and J. Tang, "Single image dehazing via conditional generative adversarial network," in *IEEE CVPR*, 2018, pp. 8202–8211.

[7] C. Ancuti, C. O. Ancuti, R. Timofte, L. Van Gool, L. Zhang, M. Yang, V. M. Patel, H. Zhang, V. A. Sindagi, R. Zhao, X. Ma, Y. Qin, L. Jia, K. Friedel, S. Ki, H. Sim, J. Choi, S. Kim, S. Seo, S. Kim, M. Kim, R. Mondal, S. Santra, B. Chanda, J. Liu, K. Mei, J. Li, Luyao, F. Fang, A. Jiang, X. Qu, T. Liu, P. Wang, B. Sun, J. Deng, Y. Zhao, M. Hong, J. Huang, Y. Chen, E. Chen, X. Yu, T. Wu, A. Genc, D. Engin, H. K. Ekenel, W. Liu, T. Tong, G. Li, Q. Gao, Z. Li, D. Tang, Y. Chen, Z. Huo, A. Alvarez-Gila, A. Galdran, A. Bria, J. Vazquez-Corral, M. Bertalmo, H. S. Demir, O. F. Adil, H. X. Phung, X. Jin, J. Chen, C. Shan, and Z. Chen, "Ntire 2018 challenge on image dehazing: Methods and results," in *IEEE CVPR Workshops*, 2018, pp. 1004–100 410.

[8] Y. Zhang, L. Ding, and G. Sharma, "HazeRD: An outdoor scene dataset and benchmark for single image dehazing," in *IEEE ICIP*, 2017, pp. 3205–3209.

[9] D. Berman, T. Treibitz, and S. Avidan, "Single image dehazing using haze-lines," *IEEE TPAMI*, vol. 42, no. 3, pp. 720–734, 2020.

[10] Y. Dong, Y. Liu, H. Zhang, S. Chen, and Y. Qiao, "FD-GAN: Generative adversarial networks with fusion-discriminator for single image dehazing," in *AAAI*, vol. 34, no. 07, 2020, pp. 10 729–10 736.

[11] B. Li, X. Peng, Z. Wang, J. Xu, and D. Feng, "AOD-Net: All-in-one dehazing network," in *IEEE ICCV*, 2017, pp. 4780–4788.